Subsalt imaging with internal multiples

Alison E. Malcolm, Department of Earth, Atmospheric and Planetary Sciences, MIT, Bjørn Ursin, Department of Petroleum Engineering and Applied Geophysics, Norwegian University of Science and Technology, and Maarten V. de Hoop, Center for Computational and Applied Mathematics and Geo-Mathematical Imaging Group, Purdue University*

SUMMARY

If singly scattered seismic waves illuminate the entirety of a subsurface structure of interest, standard methods can be applied to image it. In many cases, subsalt imaging for example, a combination of restricted acquisition geometry and imperfect velocity models results in regions of the model that are not illuminated with singly scattered waves. We present an approach to use multiply scattered waves to illuminate such structures, and illustrate the method by creating images of the base of salt with an erroneous velocity model. This method builds upon past work in which methods to predict artifacts in imaging from multiply scattered waves have been developed and shares similarities with current techniques of imaging with surface-related multiples.

INTRODUCTION

In this paper we discuss a method for subsalt imaging using internal multiples. Our approach extends the work of Malcolm and de Hoop (2005) by including illumination in a series representation that models the data as a superposition of different phases. By explicitly including illumination in the series representation we identify those multiples which carry information about regions of the subsurface not illuminated by singly scattered waves.

Imaging with internal multiples in the framework of the one-way wave equation requires a "multi-pass" approach reminiscent of the generalized Bremmer series (de Hoop, 1996). Turning waves are accounted for in such an approach as discussed by Xu and Jin (2006); Zhang et al. (2006); see also Hale et al. (1991). In the multi-pass approach, starting at the surface (or top), waves are first propagated downwards and then stored at each depth; in the second "pass", starting at the bottom, reflection operators derived from the estimated standard image are applied to the stored fields and the results are propagated, accumulatively, back upwards. For turning waves, or doubly scattered waves this up-going field is correlated with the saved down-going field to form an image of steeply-dipping reflectors (for doubly scattered waves this is similar to the work of Jin et al. (2006); Xu and Jin (2007)). For internal multiples the source-side up-going field is correlated with the receiver-side up-going field to form an image of e.g. the base of salt. A related method for imaging with surface-related multiples has been proposed by Berkhout & Verschuur (1994; 2006) in which one leg of the surface multiple generates a new primary wave with the source at the surface reflection point; similar techniques are also discussed in Guitton (2002). Another method for imaging with surface-related multiples with particular emphasis on reducing cross-talk between the two (or more) images is given in Brown and Guitton (2005). For surface-related multiples, this improves the range of scattering angles illuminated for a single data set and allows the imaging of a larger region. Interferometric techniques can be applied to multiples to allow standard migration techniques to be applied to the resulting data; this is discussed in Schuster et al. (2004); Jiang (2006); Jiang et al. (2007); Vasconcelos et al. (2007). Here we use internal multiples, recorded at the surface, to image around complicated structures, such as salt domes, to create an image of the base of salt using waves that have not passed through it.

Our series approach builds on the development of the inverse generalized Bremmer coupling series in Malcolm and de Hoop (2005) which combines aspects of the Lippmann-Schwinger equation driven inverse scattering series developed by Weglein *et al.* (1997; 2003) with the generalization of the Bremmer series (Bremmer, 1951) developed by De Hoop (1996).

THEORY

Following past work on artifact prediction (Malcolm and de Hoop, 2005; Malcolm et al., 2007), we define the matrices

$$\mathsf{G} = \begin{pmatrix} G_+ & 0 \\ 0 & G_- \end{pmatrix}, \tag{1}$$

where G_+ propagates waves upward and G_- downward and

$$\widehat{V} = \begin{pmatrix} \widehat{V}_{++} & \widehat{V}_{+-} \\ \widehat{V}_{-+} & \widehat{V}_{--} \end{pmatrix}, \tag{2}$$

where $\widehat{V}$ is the so-called contrast operator that governs the coupling of wave components. The $\widehat{V}$ operator is decomposed into a series $\widehat{V} = \Sigma_{j=1}^{M} \widehat{V}_j$ with $\widehat{V}_j$ representing the j^{th} order in the data contrast similar to Weglein et al. (2003). In this formulation, $\widehat{V}_{-+}$ couples down to up-going waves, $\widehat{V}_{--}$ up to up-going waves etc. To account for illumination, we then take the first-order contrast, $\widehat{V}_1$ and split it into three parts via

$$\widehat{V}_1 = \widehat{V}_1' + \widehat{V}_1'' + \widehat{V}_1''' + \ldots, \tag{3}$$

where $\widehat{V}_1'$ is the part of the model that has been illuminated by the recorded singly scattered data, $\widehat{V}_1''$ is the part of the model that is first illuminated by the doubly scattered data, $\widehat{V}_1'''$ is the part of the model first illuminated by triply scattered data, and so on.

From the recursions given in (Malcolm and de Hoop, 2005,equations (52-54)) and the above series for $\widehat{V}_1$ in equation (3) we can derive an expression for the scattered field and from this an equation modeling the data. The scattered field expression is complicated, however, by the appearance of wave-paths such as those illustrated in Figure 1 (c-e). Assuming a standard seismic acquisition geometry where the sources and receivers are restricted to the Earth's surface allows the derivation of the much simpler data equation

$$\begin{aligned} d = \mathsf{R}\, Q_-^*\, \partial_t^2 G_- \Big[& (\widehat{V}_1')_{-+} + \partial_t^2 (\widehat{V}_1')_{-+}\, G_+\, (\widehat{V}_1'')_{++} \\ & + \partial_t^2 (\widehat{V}_1'')_{--}\, G_-\, (\widehat{V}_1')_{-+} + \partial_t^4 (\widehat{V}_1')_{-+}\, G_+\, (\widehat{V}_1''')_{+-}\, G_-\, (\widehat{V}_1')_{-+} \Big]\, G_+ f_+, \end{aligned} \tag{4}$$

where d are the data, R restricts the resulting wavefield to $z = 0$, f_+ is a source of down-going energy, and Q_-^* is introduced by Stolk and de Hoop (2006) and forms a part of the recomposition of the up and down-going wavefields to form the total wavefield. In equation (4) the first term represents primaries, the second doubly scattered waves or prismatic reflections, and the third multiples. In the following section, we present our proposed algorithm to image from this equation using multiply scattered waves.

ALGORITHM

We start with the data equation (4). Our imaging strategy is as follows. We "project" d onto d_1 where

$$d_1 = \mathsf{R}\, Q_-^*\, \partial_t^2 G_- ((\widehat{V}_1')_{-+} (G_+ f_+)) \tag{5}$$

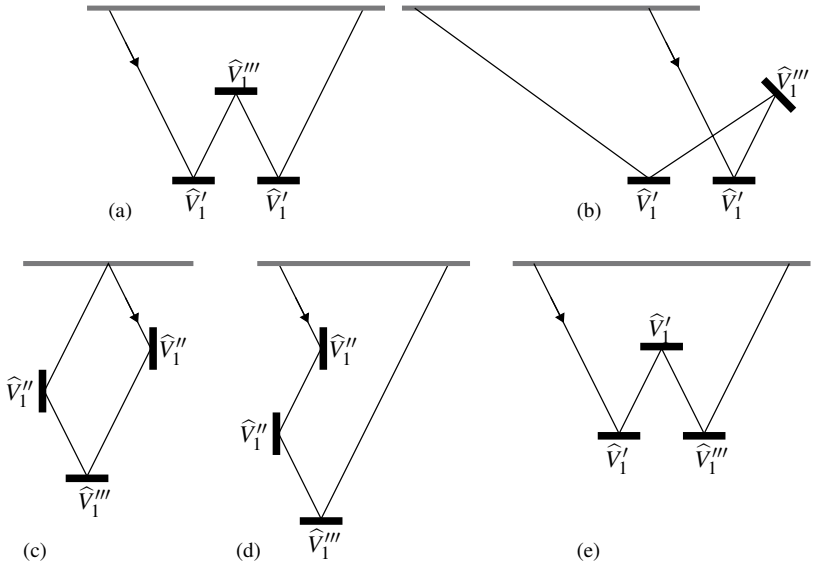

Figure 1: Illustration of some of the wavepaths that could contribute to the data and their relationship to the illumination decomposition of $\widehat{V}$ into $\widehat{V}'$,$\widehat{V}''$, and $\widehat{V}'''$. (a) and (b) are included in our analysis while (c)-(e) are not.

in the range of the single scattering operator, by minimizing $\|d-d_1\|$. We then propagate these data downward and reconstruct the image $(\widehat{V}_1')_{-+}$ by applying an imaging condition. We then select a part, $(\hat{\widehat{V}}_1)_{-+}$, of this reconstruction to become a scatterer in the background model. We emphasize that this does not amount to adding a particular reflector to the velocity model as in reverse-time migration or the method proposed by Youn and Zhou (2001) but simply isolates a region of the model expected to form the deeper reflections for internal multiples; this separation also reduces the cross-talk between singly and multiply scattered images (see Brown and Guitton (2005) for a thorough discussion of cross-talk). (We suppress the mention of imaging with doubly scattered waves here as this procedure would be similar to that proposed by Jin et al. (2006); Xu and Jin (2007); however, in general the doubly scattered data should be estimated next.) We then define a composite Green's function

$$\widetilde{G}_{-+}\cdot = \partial_t^2 G_-((\hat{\widehat{V}}_1)_{-+}(G_+\cdot)), \tag{6}$$

which accounts for propagation to the reflector, reflection from it, and propagation upwards towards the second scattering point. We proceed with "projecting" $d-d_1-d_2$ onto d_3 in the range of the "triple" scattering scattering operator, (substituting (6) into the third term of equation (4))

$$d_3 = \mathsf{R}\mathcal{Q}_-^*\partial_t^2\widetilde{G}_{-+}((\widehat{V}_1''')_{+-}(\widetilde{G}_{-+}f_+)), \tag{7}$$

by minimizing $\|(d-d_1-d_2)-d_3\|$. From equation (7) the reconstruction of $(\widehat{V}_1''')_{+-}$ is done by applying a standard imaging condition to the computed $\widetilde{G}$'s. For computational efficiency, we approximate d_3 through a time-windowing procedure, applied at depth to separate the primaries used to form $(\hat{\widehat{V}}_1)_+$ from the multiples used in estimating $(\widehat{V}_1''')_{+-}$.

This algorithm is illustrated in Figure 2. In (a)-(d) the wavefield is shown to highlight the different arrivals included in our imaging procedure. In the algorithm, first 'D', the direct wave, is simulated as in standard shot migration; from the standard image made as this wavefield is propagated, an estimate of the location of the lower reflector (at 1.5 km marked with a solid line) is made. Using this estimated image, the reflected wave 'R' is simulated from the source side. Concurrently the same procedure is applied to the data, propagating them first down and then up after interacting with the lower reflector through $\hat{\widehat{V}}_1$. In Figure 2(e) singly, doubly and triply scattered waves are used to form an image of the cube from the outside assuming a constant background velocity. To image the sides of the cube with doubly scattered waves, we apply an imaging condition to the downgoing wavefield 'D' on the source (receiver) side and the reflected wavefield 'R' on the receiver (source) side. To image the bottom of the cube with multiples, we use the 'R' wavefield from both the source and receiver sides. In (f) and (g) we compare the accuracy of the location of the lower edge of the cube, migrating with a constant background velocity, using primaries (imaging from above) and multiples (imaging from below). Because the multiples do not pass through the cube they give a more accurate location of its lower edge.

EXAMPLES

To test the ability of the above described theory to image the base of salt, we developed a model in which the salt contains sediment inclusions; we then study the influence of these inclusions on the location of the bottom of salt both with singly and triply scattered waves. We generated 2D finite difference data in two models: the 'inclusion model' and the 'inclusion-free model'. The inclusion model is shown in Figure 3 (a); the inclusion-free model differs only in the absence of the inclusions.

In Figure 3 (b) a standard image is made with the inclusion model. Because the velocity model is correct in this case, the base of salt is well imaged. In Figure 3 (c) the inclusion data are migrated through the inclusion-free model, resulting in a much poorer image of the base of the salt.

In Figure 4 we illustrate imaging with multiples. In Figure 4(a) an image is made of the base of salt in the inclusion-free model using waves that have passed through the salt. This results in an image of the base of salt that is comparable to the single-scattered image indicating that as good an image is possible with multiples as with primaries when the salt structure is known. In Figure 4(b) an image is made, again in the inclusion-free model, restricting the wavepaths to not have

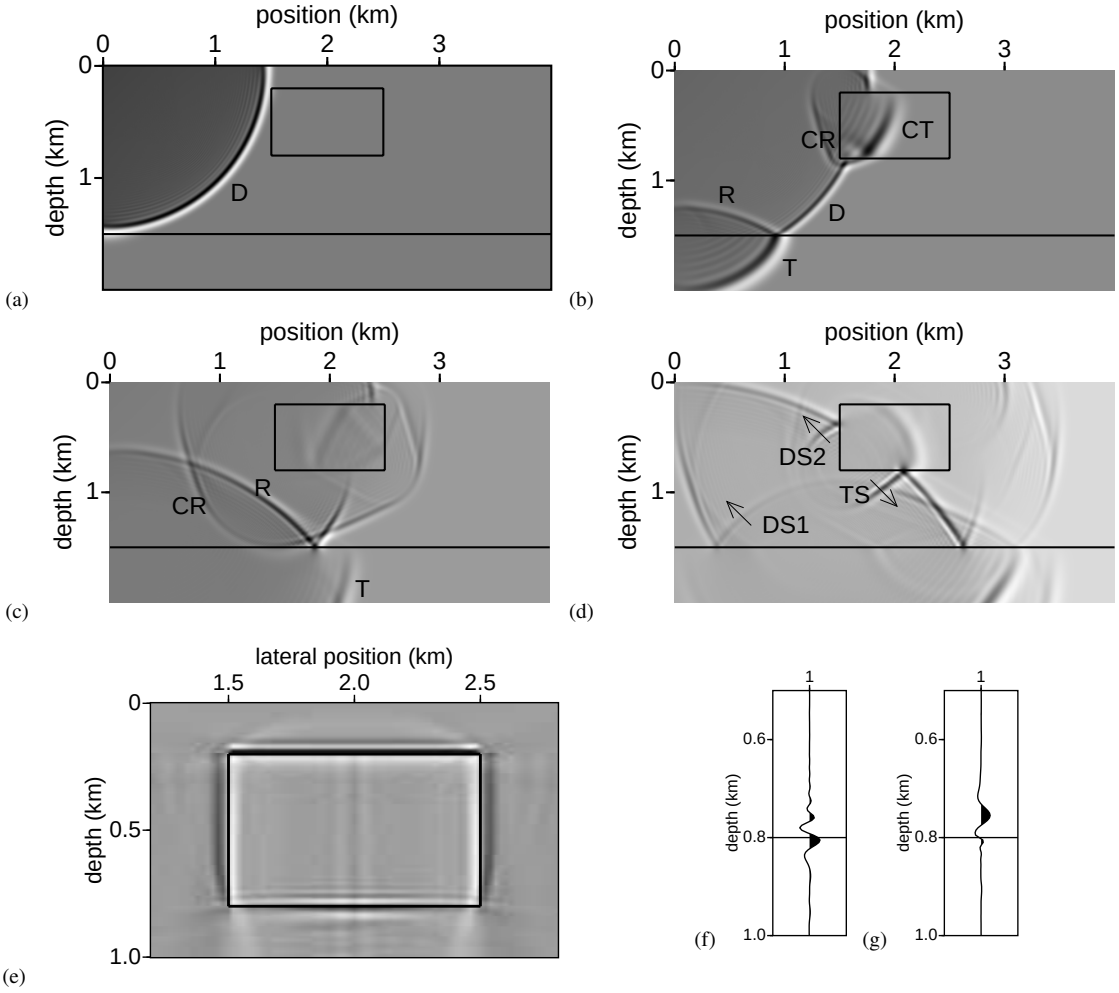

Figure 2: Using multiply scattered energy allows the full illumination of an object of interest from surface data. Here we illustrate both the data that are used in the imaging and the resultant images. In (a) through (d) we show snapshots of the wavefield, with time increasing from (a) to (d), as the data are generated. The annotations on the plots highlight different phases used in imaging; 'D' is the direct (downgoing) wave, 'R' is reflected (upcoming) from the lower reflector and 'T' is transmitted through it, 'CR' is the constituent reflected from the cube and 'CT' is the constituent transmitted into it, 'DS1' and 'DS2' are the doubly scattered waves off the left vertical edge of the cube and 'TS' is the underside reflection. In all plots the solid lines mark the positions of reflectors. In (e) we show an image, made assuming constant background velocity, of the cube structure; the vertical edges are imaged with doubly scattered waves ('DS1' and 'DS2' in (d)) and the bottom with triply scattered waves ('TS' in (d)). In (f) and (g) we show that imaging with triply scattered waves – and a constant background velocity – locates the reflector at the correct depth (in (f)), whilst imaging from above, shown in (g), naturally places the reflector at the wrong depth. The traces in (f) and (g) are stacks of images at the base of the cube; the solid line marks the correct reflector location.

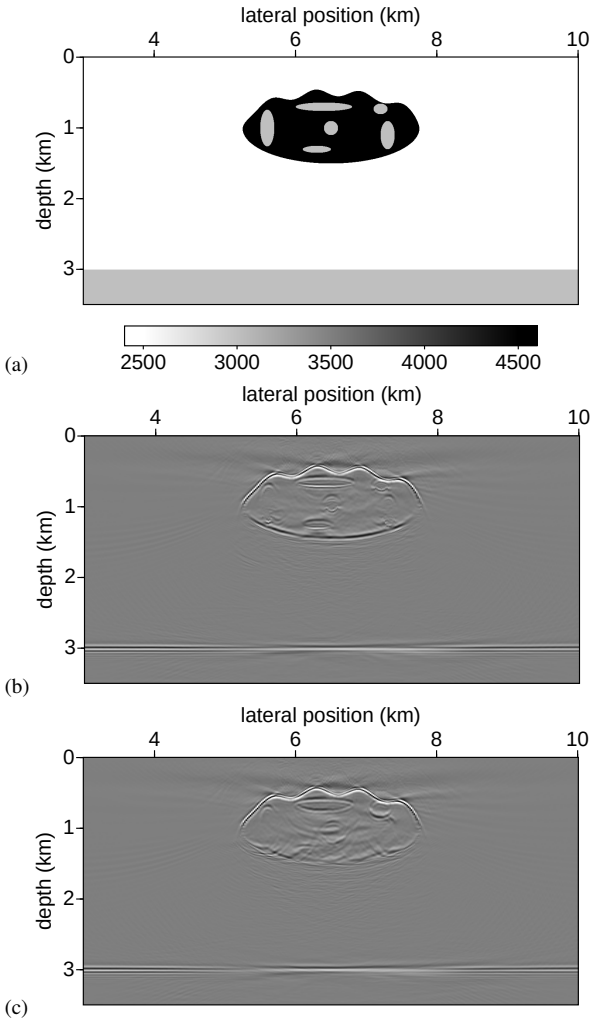

Figure 3: (a) Velocity model for the salt example; (b) Image made with inclusion data and velocity model; (c) Image made with the inclusion data and the inclusion-free velocity model.

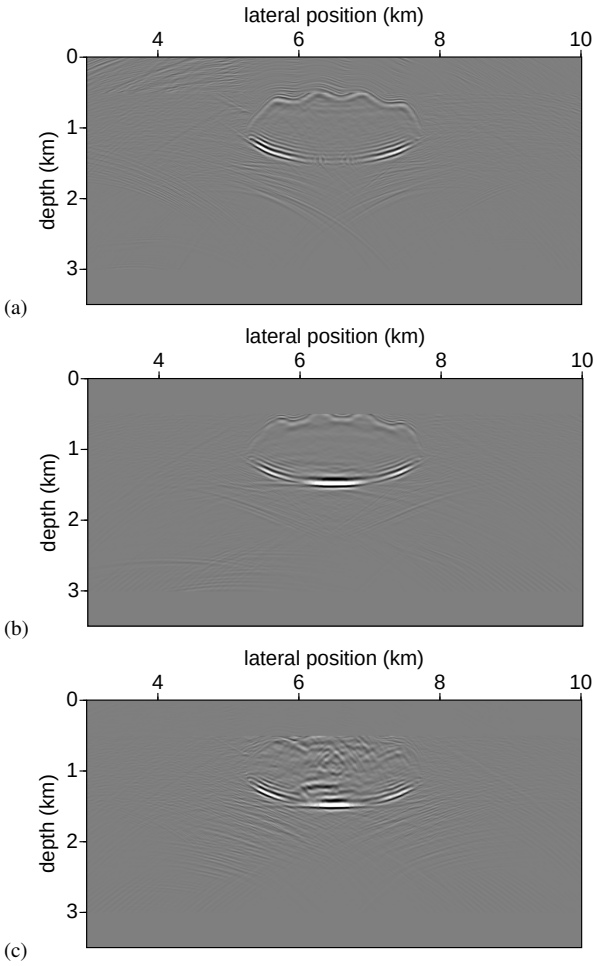

Figure 4: (a) When the salt structure is known, waves passing through it can be used to make an image of the base of salt that is comparable to a standard image; this image is made with data from the inclusion-free model. (b) Underside multiple image with data from the no-inclusion model. (c) Underside multiple image made with data from the inclusion model, migrated with the inclusion-free velocity; because waves do not travel through the salt the image is nearly as good as the inclusion-free case in (b).

passed through the salt by limiting the source and receiver positions contributing to each region of the image. In this case, the flanks are imaged with wave paths as in Figure 1(a) and the base with paths as in Figure 1(b). In Figure 4(c) we show an image made with the same method as in Figure 4(b) but with data from the inclusion model (the imaging was still performed in the inclusion-free velocity model). This image is comparable to the inclusion-free case because little energy passes through the (erroneous) salt structure in the formation of the image.

CONCLUSIONS

Multiply scattered waves have the ability to contribute useful information to seismic images. Because they illuminate structures not easily illuminated by primaries, these waves allow the imaging of regions of the Earth not illuminated by singly scattered waves. By including the illumination footprint of the acquisition geometry from the beginning of our, series based, data representation we are able to isolate the contributions from different orders of scattering. Once these contributions are isolated it is possible to develop an algorithm to treat each order of multiple scattering separately. It is important to note, however, that the resulting algorithms are quite similar and can in fact be combined into one multiple-scattering imaging algorithm. Through synthetic examples, we have illustrated that including multiply scattered waves in the imaging process enhances our ability to image the under side of complicated structures such as salt domes.

ACKNOWLEDGMENTS

Much of this work was done while AM was a postdoc at Utrecht University supported by the Dutch National Science Foundation grant number NWO:VIVI865.03.007. BU would like to acknowledge financial support from StatoilHydro and the Norwegian Research Council through the ROSE project. MVdH was supported in part by the members of the Geo-Mathematical Imaging Group.

EDITED REFERENCES

Note: This reference list is a copy-edited version of the reference list submitted by the author. Reference lists for the 2008 SEG Technical Program Expanded Abstracts have been copy edited so that references provided with the online metadata for each paper will achieve a high degree of linking to cited sources that appear on the Web.

REFERENCES

Berkhout, A. J., and D. J. Vershuur, 1994, Multiple technology: Part 2 migration of multiple reflections: 64th Annual International Meeting, SEG, Expanded Abstracts, 1497–1500.

———2006, Imaging of multiple reflections: Geophysics, **71**, SI209–SI220.

Bremmer, H., 1951, The W. K. B. approximation as the first term of a geometric-optical series: Communications on Pure and Applied Mathematics, **4**, 105–115.

Brown, M. P., and A. Guitton, 2005, Least-squares joint imaging of multiples and primaries: Geophysics, **70**, S79–S89.

de Hoop, M. V., 1996, Generalization of the Bremmer coupling series: Journal of Mathematical Physics, **37**, 3246–3282.

Guitton, A., 2002, Shot-profile migration of multiple reflections: 72nd Annual International Meeting, SEG, Expanded Abstracts, 1296–1299.

Hale, D., N. R. Hill, and J. P. Stefani, 1991, Imaging salt with turning seismic waves: 61st Annual International Meeting, SEG, Expanded Abstracts, 1171–1174.

Jiang, Z., 2006, Migration of interbed multiple reflections: 76th Annual International Meeting, SEG, Expanded Abstracts, 3501–3505.

Jiang, Z., J. Sheng, J. Yu, G. T. Schuster, and B. E. Hornby, 2007, Migration methods for imaging different-order multiples: Geophysical Prospecting, **55**, 1–19.

Jin, S., S. Xu, and D. Walraven, 2006, One-return wave equation migration: Imaging of duplex waves: 76th Annual International Meeting, SEG, Expanded Abstracts, 2338–2342.

Malcolm, A. E., and M. V. de Hoop, 2005, A method for inverse scattering based on the generalized Bremmer coupling series: Inverse Problems, **21**, 1137–1167.

Malcolm, A. E., M. V. de Hoop, and H. Calandra, 2007, Identification of image artifacts from internal multiples: Geophysics, **72**, S123–S132.

Schuster, G. T., J. Yu, J. Sheng, and J. Rickett, 2004, Interferometric/daylight seismic imaging: Geophysical Journal International, **157**, 838–852.

Stolk, C. C., and M. V. de Hoop, 2006, Seismic inverse scattering in the downward continuation approach: Wave Motion, **43**, 579–598.

Vasconcelos, I., R. Snieder, and B. Hornby, 2007, Target-oriented interferometry—Imaging with internal multiples from subsalt VSP data: 77th Annual International Meeting, SEG, Expanded Abstracts, 3069–3073.

Weglein, A., F. B. Araujo, P. M. Carvalho, R. H. Stolt, K. H. Matson, R. T. Coates, D. Corrigan, D. J. Foster, S. A. Shaw, and H. Zhang, 2003, Inverse scattering series and seismic exploration: Inverse Problems, **19**, R27–R83.

Weglein, A., F. A. Gasparotto, P. M. Carvalho, and R. H. Stolt, 1997, An inverse-scattering series method for attenuating multiples in seismic reflection data: Geophysics, **62**, 1975–1989.

Xu, S., and S. Jin, 2006, Wave equation migration of turning waves: 76th Annual International Meeting, SEG, Expanded Abstracts, 2328.

———2007, An orthogonal one-return wave-equation migration: 77th Annual International Meeting, SEG, Expanded Abstracts, 2325–2329.

Youn, O. K., and H. Zhou, 2001, Depth imaging with multiples: Geophysics, **66**, 246–255.

Zhang, Y., S. Xu, and G. Zhang, 2006, Imaging complex salt bodies with turning-wave one-way wave equation: 76th Annual International Meeting, SEG, Expanded Abstracts, 2323.